

MIT Open Access Articles

Charmonium production in pNe collisions at $\sqrt{s_{NN}} = 68.5$ GeV

The MIT Faculty has made this article openly available. **Please share** how this access benefits you. Your story matters.

Citation: The European Physical Journal C. 2023 Jul 17;83(7):625

As Published: <https://doi.org/10.1140/epjc/s10052-023-11608-6>

Publisher: Springer Berlin Heidelberg

Persistent URL: <https://hdl.handle.net/1721.1/151164>

Version: Final published version: final published article, as it appeared in a journal, conference proceedings, or other formally published context

Terms of use: Creative Commons Attribution





Charmonium production in p Ne collisions at $\sqrt{s_{NN}} = 68.5$ GeV

LHCb Collaboration*

CERN, 1211 Geneva 23, Switzerland

Received: 23 November 2022 / Accepted: 12 May 2023
© CERN for the benefit of the LHCb collaboration 2023

Abstract The measurement of charmonium states produced in proton-neon (p Ne) collisions by the LHCb experiment in its fixed-target configuration is presented. The production of J/ψ and $\psi(2S)$ mesons is studied with a beam of 2.5 TeV protons colliding on gaseous neon targets at rest, corresponding to a nucleon-nucleon centre-of-mass energy $\sqrt{s_{NN}} = 68.5$ GeV. The data sample corresponds to an integrated luminosity of 21.7 ± 1.4 nb $^{-1}$. The J/ψ and $\psi(2S)$ hadrons are reconstructed in $\mu^+\mu^-$ final states. The J/ψ production cross-section per target nucleon in the centre-of-mass rapidity range $y^* \in [-2.29, 0]$ is found to be $506 \pm 8 \pm 46$ nb/nucleon. The ratio of J/ψ and D^0 cross-sections is evaluated to $(1.06 \pm 0.02 \pm 0.09)\%$. The $\psi(2S)$ to J/ψ relative production rate is found to be $(1.67 \pm 0.27 \pm 0.10)\%$ in good agreement with other measurements involving beam and target nuclei of similar sizes.

The production of charmonia, $c\bar{c}$ bound states, is interesting to study in proton-proton, proton-nucleus and nucleus-nucleus collisions. This process involves two scales: that of the $c\bar{c}$ pair production, which can be studied in proton-proton collisions; and that of hadronization, for which proton-nucleus collisions can bring decisive insights.

Several initial- and final-state effects occur in proton-nucleus collisions that can modify charmonium production with respect to proton-proton collisions. Charmonium production can be suppressed by nuclear absorption [1] and can be affected by multiple scattering [2], and energy loss by radiation [3] in the proton-nucleus overlapping region. Charmonium states can also be dissociated by comovers [4] or affected by the modification, namely shadowing or anti-shadowing, of the parton flux inside the nucleus [5,6]. These so-called cold nuclear-matter effects (CNM) depend on the collision energy, the transverse momentum and rapidity of the produced charmonium state, as well as the size of the target nucleus. It is therefore essential to carry out charmonium measurements over a wide range of experimental conditions. Moreover, the understanding of charmonium production and

hadronization mechanisms can be significantly improved by comparison with measurements of the overall charm quark production, for which D^0 mesons are a good proxy, as their production dominates over other charm hadrons.

In this paper, a measurement of charmonium production in the LHCb fixed-target configuration is presented. The production of J/ψ mesons is studied in collisions of protons with energies of 2.5 TeV incident on neon nuclei at rest, resulting in centre-of-mass energies of $\sqrt{s_{NN}} = 68.5$ GeV. It is also compared with the production of D^0 mesons measured in the same conditions [7]. In addition, the first measurement of the relative production rate of $\psi(2S)$ and J/ψ mesons in this fixed-target configuration is reported.

The LHCb detector [8,9] is a single-arm forward spectrometer covering the pseudorapidity range $2 < \eta < 5$. It was designed primarily for the study of particles containing c or b quarks. The main detector elements are: the silicon-strip vertex locator (VELO) surrounding the interaction region that allows to precisely reconstruct the decay vertex of c and b hadrons; a tracking system with a warm magnet and tracking stations that provide a measurement of the momentum of charged particles; two ring-imaging Cherenkov detectors that provide discrimination between different species of charged hadrons; a calorimeter system consisting of scintillating-pad and preshower detectors in front of the electromagnetic and hadronic calorimeters; and a muon detector composed of alternating layers of iron and multiwire proportional chambers. The system for measuring the overlap with gas (SMOG) [10,11] is used to measure LHC beam profiles. It enables the injection of gases with pressure of $O(10^{-7})$ mbar in the beam-pipe section inside the VELO, allowing LHCb to operate as a fixed-target experiment. SMOG allows the injection of noble gases and therefore gives the unique opportunity to study nucleus-nucleus and proton-nucleus collisions on various targets. Due to the boost induced by the high-energy proton beam, the LHCb acceptance covers the backward rapidity hemisphere in the nucleon-nucleon centre-of-mass system of the reaction, $-2.29 < y^* < 0$.

* e-mail: fleuret@in2p3.fr

Events are selected by the two-stage trigger system [12]. The first level is implemented in hardware and uses information provided by the calorimeters and the muon detectors, while the second is a software trigger. The hardware trigger requires at least one identified muon for the reconstruction of the $J/\psi \rightarrow \mu^+\mu^-$ and $\psi(2S) \rightarrow \mu^+\mu^-$ decays. The software trigger requires two well-reconstructed muons having an invariant mass, $m_{\mu^+\mu^-}$, greater than $2700 \text{ MeV}/c^2$.

The data samples correspond to a collider configuration in which proton bunches moving towards the detector do not cross any bunch moving in the opposite direction. Unlike in proton-proton (pp) collisions, no nominal interaction point exists in the fixed-target case. Therefore, events are required to have a reconstructed primary vertex (PV) with its coordinate along the beam axis (z) being within the fiducial region $z_{PV} \in [-200, -100] \cup [100, 150] \text{ mm}$ (where $z_{PV} = 0 \text{ mm}$ is the nominal position of the pp interaction point), within which high reconstruction efficiencies are achieved and calibration samples are available. Residual pp collision events, are suppressed by vetoing events with activity in the backward direction with respect to the beam direction, based on the number of hits in VELO stations upstream of the interaction region. The region $-100 < z_{PV} < 100 \text{ mm}$, where most of the residual pp collisions occur, is also vetoed.

The offline selections of J/ψ and $\psi(2S)$ candidates are similar to those used in Ref. [13]. Events must contain a primary vertex with at least four tracks reconstructed in the VELO detector. The J/ψ and $\psi(2S)$ candidates are constructed from two oppositely-charged muons forming a good-quality vertex. The well-identified muons have a transverse momentum, p_T , larger than $500 \text{ MeV}/c$ and are required to be consistent with originating from the PV, which suppresses J/ψ and $\psi(2S)$ mesons coming from b -hadron decays. The measurements are performed in the ranges of transverse momentum $p_T < 8 \text{ GeV}/c$ and rapidity $2.0 < y < 4.29$ of J/ψ and $\psi(2S)$ mesons. Corrections for the acceptance and reconstruction efficiencies are determined using samples of simulated proton-neon ($p\text{Ne}$) collisions. In the simulation, J/ψ and $\psi(2S)$ mesons are generated using PYTHIA 8 [14] with a specific LHCb configuration [15] and with colliding-proton beam momentum equal to the momentum per nucleon of the beam and target in the centre-of-mass frame. The decays are described by EVTGEN [16], in which final-state radiation is generated using PHOTOS [17]. The generated J/ψ and $\psi(2S)$ meson decay products are embedded into $p\text{Ne}$ minimum-bias events that are generated with the EPOS event generator [18] using beam parameters obtained from data. Decays of hadrons generated with EPOS are also described by EVTGEN. The interaction of the generated particles with the detector and its response are implemented using the GEANT4 toolkit [19,20] as described in Ref. [21]. After reconstruction, the simulated events are assigned weights, based on the VELO cluster multiplicity. This ensures that the event multiplicity

Table 1 Systematic and statistical uncertainties on the J/ψ meson yield. Systematic uncertainties correlated between bins affect all measurements by the same relative amount. Ranges denote the minimum and the maximum values among the y^* or p_T intervals while the latter value is the uncertainty integrated over y^* or p_T

Systematic uncertainties	
Uncorrelated between bins	
Simulation sample size	[1.4, 7.0]%; 2.3 %
Signal determination	[1.4, 11.0]%; 3.5 %
Correlated between bins	
Proton-proton collisions	2.0%
Neon purity	1.2%
Tracking efficiency	1.1%
Particle identification efficiency	1.1%
PV	3.9%
Luminosity	6.5%
Statistical uncertainty	1.6%

and the PV position follow the same distributions as in the data.

Figure 1 shows the invariant-mass distributions for the J/ψ and $\psi(2S)$ candidates, from which the corresponding signal yields are obtained with extended maximum-likelihood fits, after all selection criteria are applied to the entire $p\text{Ne}$ data set. The signals are described by Crystal Ball functions [22] and the background shapes are modelled by exponential functions. The total J/ψ and $\psi(2S)$ signal yields are 4542 ± 71 and 76 ± 12 , respectively. The signal yields are determined independently in intervals of p_T and y^* . These yields are corrected for the total efficiencies, evaluated to 36.6% and 38.8% for the J/ψ and $\psi(2S)$ respectively, which account for the geometrical acceptance of the detector, and the efficiencies of the trigger, event selection, PV and track reconstruction, and particle identification. Particle identification [23] and tracking efficiencies are obtained from control samples in pp collision data. All other efficiencies are determined using samples of simulated data.

Several sources of systematic uncertainty are considered, affecting either the determination of the signal yields or the total efficiencies. They are summarised in Table 1 separately for contributions that are correlated and uncorrelated between different intervals of p_T and y^* . Systematic uncertainty on the signal determination includes several contributions. A significant systematic uncertainty arises from the finite size of the simulation samples. The systematic uncertainty associated to the determination of the signal yields is related to the mass fit. This uncertainty is evaluated using alternative models for signal and background shapes, Gaussian and polynomial functions respectively, that reproduce the mass distributions equally well. The effect of the small (below 0.1%) residual contribution of signal from b hadrons

Fig. 1 Invariant mass distributions of (left) $J/\psi \rightarrow \mu^- \mu^+$ candidates and (right) $\psi(2S) \rightarrow \mu^- \mu^+$ candidates. The data are overlaid with the fit function

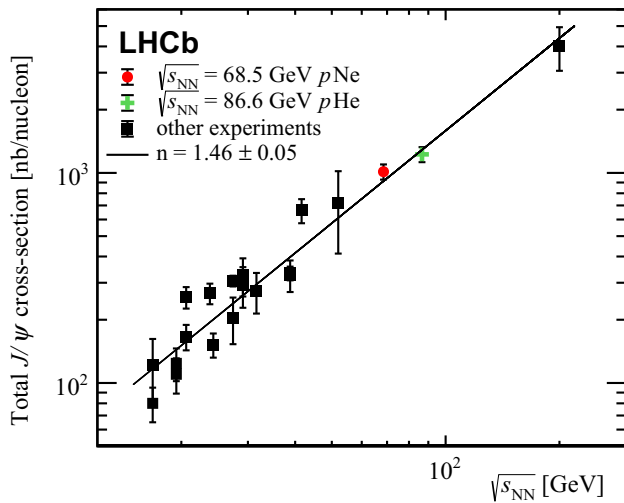
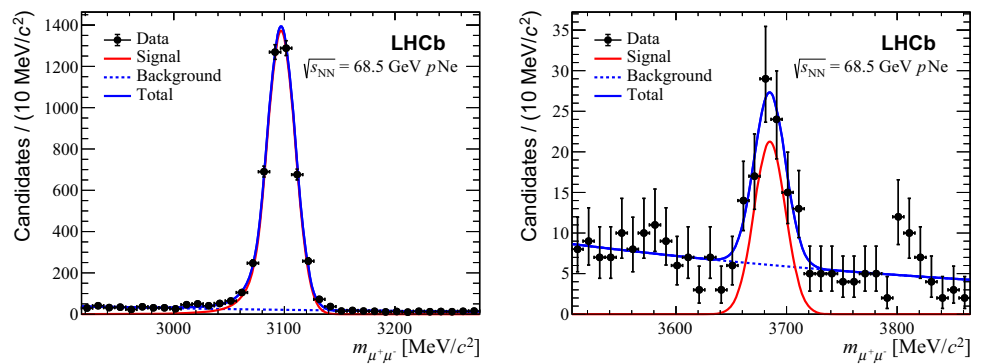


Fig. 2 Total J/ψ cross-section per target nucleon as a function of centre-of-mass energy. Experimental data, represented by black points, are taken from Ref. [24]. The red point corresponds to the p Ne result from the present analysis. The green point corresponds to a measurement performed by LHCb with p He collisions [13]

is investigated and found to be negligible. Other contributions are obtained by determining the maximum contamination from residual pp collisions with samples of pure p Ne collisions and pure pp collisions. The neon purity systematic uncertainty corresponds to the contamination from collisions between the beam and elements different from neon, coming from standard outgassing. It is quantified using data samples recorded with no neon injection. Since the tracking and particle identification efficiencies are determined using pp control samples, the differences between the track multiplicity in p Ne and pp collisions are considered as systematic uncertainties. The tracking and particle identification systematic uncertainties also take into account the size of the pp control samples. The PV reconstruction systematic uncertainty corresponds to the variation of the efficiency over the whole z_{PV} range, and to the difference between the PV reconstruction efficiency evaluated using the simulation and a data-driven approach exploiting the well-reconstructed $\phi \rightarrow K^+ K^-$ decay. The integrated luminosity is determined to be

$21.7 \pm 1.4 \text{ nb}^{-1}$ from the yield of electrons elastically scattering off the target Ne atoms as presented in Ref. [25]. The measured J/ψ production cross-section per target nucleon and within $y^* \in [-2.29, 0]$, using the world average branching fraction of $J/\psi \rightarrow \mu^+ \mu^-$ decays [26], is

$$\sigma_{J/\psi} = 506 \pm 8 \pm 46 \text{ nb/nucleon},$$

where the first uncertainty is statistical and the second systematic. To compare with previous experimental results at different energies, the J/ψ cross-section is extrapolated to the full phase space using PYTHIA 8 with the CT09MCS PDF set [27], with no additional uncertainty related to the extrapolation, assuming forward-backward symmetry in the rapidity distribution. After extrapolation, the total J/ψ cross-section is

$$\sigma_{J/\psi}^{4\pi} = 1013 \pm 16 \pm 92 \text{ nb/nucleon},$$

where the first uncertainty is statistical and the second systematic. An overview of J/ψ cross-section measurements performed at different centre-of-mass energies by different experiments [24], including this measurement and the previous LHCb measurement in p He collisions at $\sqrt{s_{NN}} = 86.6 \text{ GeV}$ [13], is shown in Fig. 2. The data are well reproduced with the function $\sigma_{J/\psi} = C \times (\sqrt{s_{NN}})^n$, with $n = 1.46 \pm 0.05$ ($\chi^2/n_{\text{dof}} = 64.6/18$ and $p\text{-value} = 4 \times 10^{-7}$), indicating a power-law dependence of the cross-section on the centre-of-mass energy, between $\sqrt{s_{NN}} \sim 20 \text{ GeV}$ and $\sqrt{s_{NN}} = 200 \text{ GeV}$.

The J/ψ differential cross-sections per target nucleon, as functions of y^* and p_T , are shown in Fig. 3. These results are compared with predictions of the HELAC-Onia (HO) generator [28–30], using QCD leading order (LO) calculations within the Color Singlet Model (CSM), with the proton CT14NLO and nuclear nCTEQ15 PDF [31] sets. The error band is obtained by varying the renormalization and factorization scales from 0.5 to 2. These predictions underestimate the measured total cross-sections. The data are better described by alternative predictions (Vogt), using calculations in the Color Evaporation Model carried out at next-to-

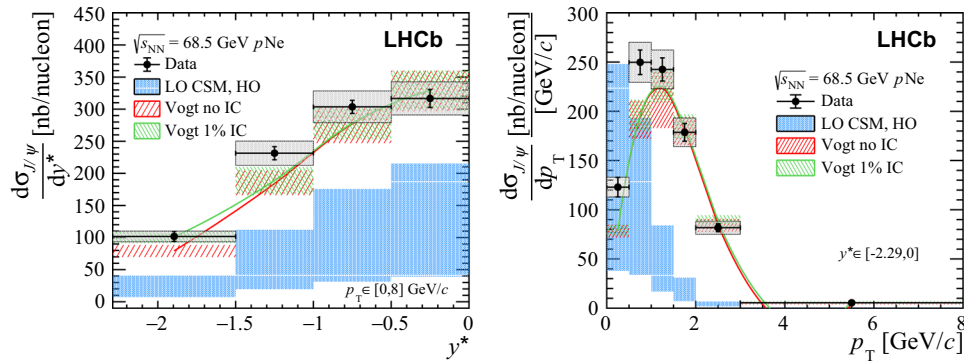
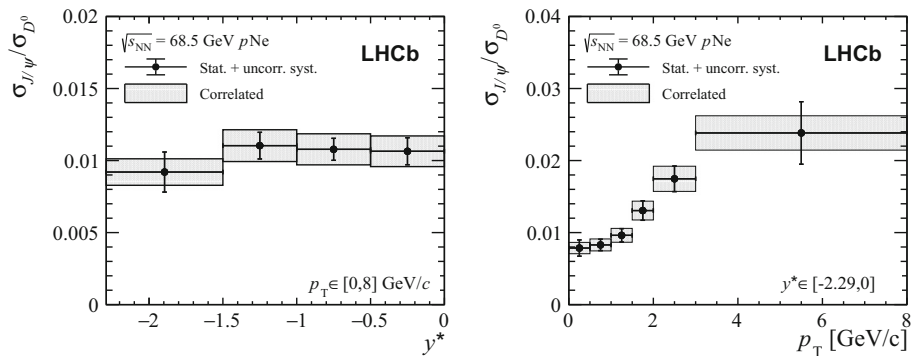


Fig. 3 Differential J/ψ cross-section as a function of (left) y^* and (right) p_T . The quadratic sums of statistical and uncorrelated systematic uncertainties are given by the error bars, while the grey boxes represent the correlated systematic uncertainties. Blue boxes (LO CSM,

HO) correspond to predictions using the CT14NLO and nCTEQ15 PDF sets [28–31]. Green and red boxes correspond to predictions (Vogt) from [32] with and without a 1% intrinsic charm (IC) contribution respectively (green and red lines indicate the central values)

Fig. 4 Ratio of J/ψ and D^0 cross-sections as a function of (left) y^* and (right) p_T . The quadratic sums of the statistical and uncorrelated systematic uncertainties are given by the error bars, while the grey boxes represent the correlated systematic uncertainties



leading order (NLO) in the heavy-flavour cross-section, with or without a 1% intrinsic charm (IC) contribution [32].

The J/ψ production cross-section is also compared to the D^0 production cross-section extracted from the same dataset, in the same kinematical conditions [7]. Several systematic uncertainties cancel in the $J/\psi/D^0$ cross-section ratio, related to the PV and track reconstruction efficiencies, the contamination from residual pp collisions, the neon purity and the luminosity determination. The ratio of J/ψ and D^0 cross-sections is

$$\frac{\sigma_{J/\psi}}{\sigma_{D^0}} = (1.06 \pm 0.02 \pm 0.09)\%$$

where the first uncertainty is statistical and the second systematic. The ratio takes into account the branching fractions [26] of $J/\psi \rightarrow \mu^+\mu^-$ and $D^0 \rightarrow K^-\pi^+$. The J/ψ -to- D^0 cross-section ratio as a function of y^* and p_T is shown in Fig. 4. Although this ratio shows a strong dependence on p_T , the data show no significant rapidity dependence.

The $\psi(2S)$ production cross-section is also measured. Due to the limited size of the $\psi(2S)$ sample, only the relative production rate of $\psi(2S)$ and J/ψ mesons is presented, where most of the efficiencies and systematic uncertainties cancel out. The remaining systematic uncertainties are evaluated to

be 0.01% for the finite size of the simulation sample, 0.09% for the total efficiency differences between J/ψ and $\psi(2S)$ and 0.05% for the signal extraction. The relative production rate of $\psi(2S)$ and J/ψ mesons is

$$\frac{\mathcal{B}_{\psi(2S) \rightarrow \mu^+\mu^-}}{\mathcal{B}_{J/\psi \rightarrow \mu^+\mu^-}} \times \frac{\sigma_{\psi(2S)}}{\sigma_{J/\psi}} = (1.67 \pm 0.27 \pm 0.10)\%$$

where $\mathcal{B}_{\psi(2S) \rightarrow \mu^+\mu^-}$ and $\mathcal{B}_{J/\psi \rightarrow \mu^+\mu^-}$ are the branching fractions of $\psi(2S) \rightarrow \mu^+\mu^-$ and $J/\psi \rightarrow \mu^+\mu^-$ decays, respectively, and the first uncertainty is statistical and the second systematic. Figure 5 compares this result to measurements performed at various centre-of-mass energies by other experiments as a function of the target atomic mass number A [33–37]. Measurement is in agreement with other proton-nucleus measurements at similar values of A .

In summary, the study of charmonium production in pNe collisions at $\sqrt{s_{NN}} = 68.5$ GeV recorded by the LHCb experiment is presented. The J/ψ production cross-section is measured in the centre-of-mass rapidity range $y^* \in [-2.29, 0]$. The comparison of this new measurement with earlier data supports a power-law dependence of the J/ψ production cross-section on centre-of-mass energy. The J/ψ -to- D^0 cross-section ratio is found to be independent of rapidity and the $\psi(2S)$ -to- J/ψ cross-section ratio is found to be

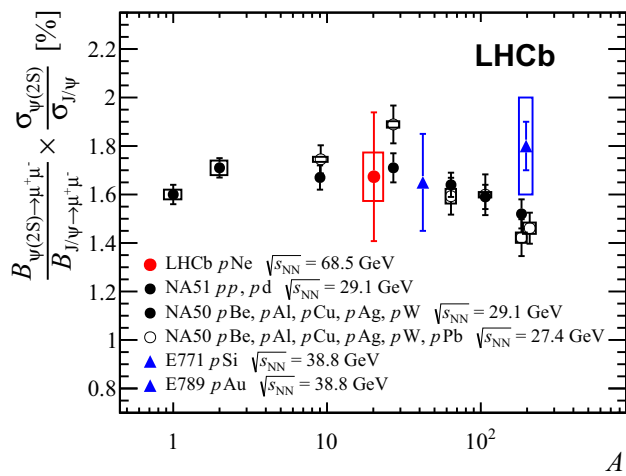


Fig. 5 The $\psi(2S)$ -to- J/ψ production ratio as a function of the target atomic mass number A . The red point corresponds to the $\sqrt{s_{NN}} = 68.5$ GeV p Ne result from the present analysis, vertical error bar corresponds to the statistical uncertainty and the box to the systematic uncertainty. The other points show previous fixed-target experimental data at various centre-of-mass energies [33–37]

$(1.67 \pm 0.27 \pm 0.10)\%$. This result is in a good agreement with other measurements involving beam and target nuclei of similar sizes, and performed at different centre-of-mass energies.

Acknowledgements We express our gratitude to our colleagues in the CERN accelerator departments for the excellent performance of the LHC. We thank the technical and administrative staff at the LHCb institutes. We acknowledge support from CERN and from the national agencies: CAPES, CNPq, FAPERJ and FINEP (Brazil); MOST and NSFC (China); CNRS/IN2P3 (France); BMBF, DFG and MPG (Germany); INFN (Italy); NWO (Netherlands); MNiSW and NCN (Poland); MEN/IFA (Romania); MICINN (Spain); SNSF and SER (Switzerland); NASU (Ukraine); STFC (United Kingdom); DOE NP and NSF (USA). We acknowledge the computing resources that are provided by CERN, IN2P3 (France), KIT and DESY (Germany), INFN (Italy), SURF (Netherlands), PIC (Spain), GridPP (United Kingdom), CSCS (Switzerland), IFIN-HH (Romania), CBPF (Brazil), Polish WLCG (Poland) and NERSC (USA). We are indebted to the communities behind the multiple open-source software packages on which we depend. Individual groups or members have received support from ARC and ARDC (Australia); Minciencias (Colombia); AvH Foundation (Germany); EPLANET, Marie Skłodowska-Curie Actions and ERC (European Union); A*MIDEX, ANR, IPhU and GLUODYNAMICS/Labex P2IO, and Région Auvergne-Rhône-Alpes (France); Key Research Program of Frontier Sciences of CAS, CAS PIFI, CAS CCEPP, Fundamental Research Funds for the Central Universities, and Sci. & Tech. Program of Guangzhou (China); GVA, XuntaGal, GENCAT and Prog. Atracción Talento, CM (Spain); SRC (Sweden); the Leverhulme Trust, the Royal Society and UKRI (United Kingdom).

Data Statement This manuscript has no associated data or the data will not be deposited. [Authors' comment: Data associated to the plots in this publication are made available on the CERN document server at <https://cds.cern.ch/record/2841849>].

Open Access This article is licensed under a Creative Commons Attribution 4.0 International License, which permits use, sharing, adaptation,

distribution and reproduction in any medium or format, as long as you give appropriate credit to the original author(s) and the source, provide a link to the Creative Commons licence, and indicate if changes were made. The images or other third party material in this article are included in the article's Creative Commons licence, unless indicated otherwise in a credit line to the material. If material is not included in the article's Creative Commons licence and your intended use is not permitted by statutory regulation or exceeds the permitted use, you will need to obtain permission directly from the copyright holder. To view a copy of this licence, visit <http://creativecommons.org/licenses/by/4.0/>.

Funded by SCOAP³. SCOAP³ supports the goals of the International Year of Basic Sciences for Sustainable Development.

References

1. C. Gerschel, J. Hüfner, A contribution to the suppression of the J/ψ meson produced in high-energy nucleus-nucleus collisions. Phys. Lett. B **207**, 253 (1988). [https://doi.org/10.1016/0370-2693\(88\)90570-9](https://doi.org/10.1016/0370-2693(88)90570-9)
2. Z.-B. Kang, J.-W. Qiu, Transverse momentum broadening of vector boson production in high energy nuclear collisions. Phys. Rev. D **77**, 114027 (2008). <https://doi.org/10.1103/PhysRevD.77.114027>
3. F. Arleo, S. Peigné, Heavy-quarkonium suppression in p-A collisions from parton energy loss in cold qcd matter. JHEP **03**, 122 (2013). [https://doi.org/10.1007/JHEP03\(2013\)122](https://doi.org/10.1007/JHEP03(2013)122). [arXiv:1212.0434](https://arxiv.org/abs/1212.0434)
4. A. Capella et al., Nonsaturation of the J/ψ suppression at large transverse energy in the comovers approach. Phys. Rev. Lett. **85**, 2080 (2000). <https://doi.org/10.1103/PhysRevLett.85.2080>. [arXiv:hep-ph/0002300](https://arxiv.org/abs/hep-ph/0002300)
5. K.J. Eskola et al., EPPS16: nuclear parton distributions with LHC data. Eur. Phys. J. C **77**, 163 (2017). <https://doi.org/10.1140/epjc/s10052-017-4725-9>. [arXiv:1612.05741](https://arxiv.org/abs/1612.05741)
6. K. Kovarik et al., NCTEQ15: global analysis of nuclear parton distributions with uncertainties in the CTEQ framework. Phys. Rev. D **93**, 085037 (2016). <https://doi.org/10.1103/PhysRevD.93.085037>. [arXiv:1509.00792](https://arxiv.org/abs/1509.00792)
7. LHCb Collaboration, R. Aaij et al., Open charm production and asymmetry in p Ne collisions at $\sqrt{s_{NN}} = 68.5$ GeV. Eur. Phys. J. C. <https://doi.org/10.1140/epjc/s10052-023-11641-5>
8. LHCb Collaboration, A.A. Alves Jr. et al., The LHCb detector at the LHC. JINST **3**, S08005 (2008). <https://doi.org/10.1088/1748-0221/3/08/S08005>
9. LHCb Collaboration, R. Aaij et al., LHCb detector performance. Int. J. Mod. Phys. A **30**, 1530022 (2015). <https://doi.org/10.1142/S0217751X15300227>. [arXiv:1412.6352](https://arxiv.org/abs/1412.6352)
10. LHCb Collaboration, R. Aaij et al., Precision luminosity measurements at LHCb. JINST **9**, P12005 (2014). <https://doi.org/10.1088/1748-0221/9/12/P12005>. [arXiv:1410.0149](https://arxiv.org/abs/1410.0149)
11. C. Barschel, Precision luminosity measurements at LHCb with beam-gas imaging. PhD thesis, RWTH Aachen University, CERN-THESIS-2013-301 (2014)
12. LHCb Collaboration, R. Aaij et al., The LHCb trigger and its performance in 2011. JINST **8**, P04022 (2013). <https://doi.org/10.1088/1748-0221/8/04/P04022>. [arXiv:1211.3055](https://arxiv.org/abs/1211.3055)
13. LHCb Collaboration, R. Aaij et al., First measurement of charm production in fixed-target configuration at the LHC. Phys. Rev. Lett. **122**, 132002 (2019). <https://doi.org/10.1103/PhysRevLett.122.132002>. [arXiv:1810.07907](https://arxiv.org/abs/1810.07907)
14. T. Sjöstrand, S. Mrenna, P. Skands, A brief introduction to PYTHIA 8.1. Comput. Phys. Commun. **178**, 852 (2008). <https://doi.org/10.1016/j.cpc.2008.01.036>. [arXiv:0710.3820](https://arxiv.org/abs/0710.3820)

15. LHCb Collaboration, I. Belyaev et al., Handling of the generation of primary events in Gauss, the LHCb simulation framework. *J. Phys. Conf. Ser.* **331**, 032047 (2011). <https://doi.org/10.1088/1742-6596/331/3/032047>
16. D.J. Lange, The EvtGen particle decay simulation package. *Nucl. Instrum. Methods A* **462**, 152 (2001). [https://doi.org/10.1016/S0168-9002\(01\)00089-4](https://doi.org/10.1016/S0168-9002(01)00089-4)
17. P. Golonka, Z. Was, PHOTOS Monte Carlo: a precision tool for QED corrections in Z and W decays. *Eur. Phys. J. C* **45**, 97 (2006). <https://doi.org/10.1140/epjc/s2005-02396-4>. [arXiv:hep-ph/0506026](https://arxiv.org/abs/hep-ph/0506026)
18. T. Pierog et al., EPOS LHC: test of collective hadronization with data measured at the CERN Large Hadron Collider. *Phys. Rev. C* **92**, 034906 (2015). <https://doi.org/10.1103/PhysRevC.92.034906>. [arXiv:1306.0121](https://arxiv.org/abs/1306.0121)
19. GEANT4 Collaboration, J. Allison et al., GEANT4 developments and applications. *IEEE Trans. Nucl. Sci.* **53**, 270 (2006). <https://doi.org/10.1109/TNS.2006.869826>
20. GEANT4 Collaboration, S. Agostinelli et al., GEANT4: a simulation toolkit. *Nucl. Instr. Methods* **506**, 250 (2003). [https://doi.org/10.1016/S0168-9002\(03\)01368-8](https://doi.org/10.1016/S0168-9002(03)01368-8)
21. M. Clemencic et al., The LHCb simulation application, Gauss: design, evolution and experience. *J. Phys. Conf. Ser.* **331**, 032023 (2011). <https://doi.org/10.1088/1742-6596/331/3/032023>
22. T. Skwarnicki, A study of the radiative cascade transitions between the Upsilon-Prime and Upsilon resonances. PhD thesis. Institute of Nuclear Physics, Krakow, DESY-F31-86-02 (1986)
23. L. Anderlini et al., The PIDCalib package, LHCb-PUB-2016-021
24. F. Maltoni et al., Analysis of charmonium production at fixed-target experiments in the NRQCD approach. *Phys. Lett. B* **638**, 202 (2006). <https://doi.org/10.1016/j.physletb.2006.05.010>. [arXiv:hep-ph/0601203](https://arxiv.org/abs/hep-ph/0601203)
25. LHCb Collaboration, R. Aaij et al., Measurement of antiproton production in p He collisions at $\sqrt{s_{NN}} = 110$ GeV. *Phys. Rev. Lett.* **121**, 222001 (2018). <https://doi.org/10.1103/PhysRevLett.121.222001>. [arXiv:1808.06127](https://arxiv.org/abs/1808.06127)
26. Particle Data Group, R.L. Workman et al., Review of particle physics. *Prog. Theor. Exp. Phys.* **2022**(8), 083C01 (2022). <https://doi.org/10.1093/ptep/ptac097>
27. H.-L. Lai et al., Parton distributions for event generators. *JHEP* **04**, 035 (2010). [https://doi.org/10.1007/JHEP04\(2010\)035](https://doi.org/10.1007/JHEP04(2010)035). [arXiv:0910.4183](https://arxiv.org/abs/0910.4183)
28. J.-P. Lansberg, H.-S. Shao, Towards an automated tool to evaluate the impact of the nuclear modification of the gluon density on quarkonium, D and B meson production in proton-nucleus collisions. *Eur. Phys. J. C* **77**, 1 (2017). <https://doi.org/10.1140/epjc/s10052-016-4575-x>. [arXiv:1610.05382](https://arxiv.org/abs/1610.05382)
29. H.-S. Shao, HELAC-Onia 2.0: an upgraded matrix-element and event generator for heavy quarkonium physics. *Comput. Phys. Commun.* **198**, 238 (2016). <https://doi.org/10.1016/j.cpc.2015.09.011>. [arXiv:1507.03435](https://arxiv.org/abs/1507.03435)
30. H.-S. Shao, HELAC-Onia: an automatic matrix element generator for heavy quarkonium physics. *Comput. Phys. Commun.* **184**, 2562 (2013). <https://doi.org/10.1016/j.cpc.2013.05.023>. [arXiv:1212.5293](https://arxiv.org/abs/1212.5293)
31. K. Kovarik et al., nCTEQ15—global analysis of nuclear parton distributions with uncertainties in the CTEQ framework. *Phys. Rev. D* **93**, 085037 (2016). <https://doi.org/10.1103/PhysRevD.93.085037>. [arXiv:1509.00792](https://arxiv.org/abs/1509.00792)
32. R. Vogt, Limits on intrinsic charm production from the SeaQuest experiment. *Phys. Rev. C* **103**, 035204 (2021). <https://doi.org/10.1103/PhysRevC.103.035204>
33. NA51 Collaboration, M.C. Abreu et al., J/ψ , ψ' and Drell–Yan production in pp and pd interactions at 450 GeV/c. *Phys. Lett. B* **438**, 35 (1998)
34. NA50 Collaboration, B. Alessandro et al., Charmonium production and nuclear absorption in p-A interactions at 450 GeV. *Eur. Phys. J. C* **33**, 31 (2004). <https://doi.org/10.1140/epjc/s2003-01539-y>
35. NA50 Collaboration, B. Alessandro et al., J/ψ and ψ' production and their normal nuclear absorption in proton-nucleus collisions at 400 GeV. *Eur. Phys. J. C* **48**, 329 (2006). <https://doi.org/10.1140/epjc/s10052-006-0079-4>. [arXiv:nucl-ex/0612012](https://arxiv.org/abs/nucl-ex/0612012)
36. E771 Collaboration, T. Alexopoulos et al., Production of J/ψ , ψ' and Υ in 800 GeV/c proton-silicon interactions. *Phys. Lett. B* **374**, 271 (1996). [https://doi.org/10.1016/0370-2693\(96\)00256-0](https://doi.org/10.1016/0370-2693(96)00256-0)
37. E789 Collaboration, M.H. Schub et al., Measurement of J/ψ and ψ' production for 800 GeV/c proton-gold collisions. *Phys. Rev. D* **52**, 1307 (1995). <https://doi.org/10.1103/PhysRevD.52.1307>

LHCb Collaboration*

R. Aaij³², A. S. W. Abdelmotteleb⁵⁰, C. Abellan Beteta⁴⁴, F. Abudinén⁵⁰, T. Ackernley⁵⁴, B. Adeva⁴⁰, M. Adinolfi⁴⁸, H. Afsharnia⁹, C. Agapopoulou¹³, C. A. Aidala⁷⁶, S. Aiola²⁵, Z. Ajaltouni⁹, S. Akar⁵⁹, K. Akiba³², J. Albrecht¹⁵, F. Alessio⁴², M. Alexander⁵³, A. Alfonso Albero³⁹, Z. Aliouche⁵⁶, P. Alvarez Cartelle⁴⁹, R. Amalric¹³, S. Amato², J. L. Amey⁴⁸, Y. Amhis^{11,42}, L. An⁴², L. Anderlini²², M. Andersson⁴⁴, A. Andreianov³⁸, M. Andreotti²¹, D. Andreou⁶², D. Ao⁶, F. Archilli¹⁷, A. Artamonov³⁸, M. Artuso⁶², E. Aslanides¹⁰, M. Atzeni⁴⁴, B. Audurier¹², S. Bachmann¹⁷, M. Bachmayer⁴³, J. J. Back⁵⁰, A. Bailly-reyre¹³, P. Baladron Rodriguez⁴⁰, V. Balagura¹², W. Baldini²¹, J. Baptista de Souza Leite¹, M. Barbetti^{22,j}, R. J. Barlow⁵⁶, S. Barsuk¹¹, W. Barter⁵⁵, M. Bartolini⁴⁹, F. Baryshnikov³⁸, J. M. Basels¹⁴, G. Bassi^{29,q}, B. Batsukh⁴, A. Battig¹⁵, A. Bay⁴³, A. Beck⁵⁰, M. Becker¹⁵, F. Bedeschi²⁹, I. B. Bediaga¹, A. Beiter⁶², V. Belavin³⁸, S. Belin⁴⁰, V. Bellee⁴⁴, K. Belous³⁸, I. Belov³⁸, I. Belyaev³⁸, G. Benane¹⁰, G. Bencivenni²³, E. Ben-Haim¹³, A. Berezhnoy³⁸, R. Bernet⁴⁴, D. Berninghoff¹⁷, H. C. Bernstein⁶², C. Bertella⁵⁶, A. Bertolin²⁸, C. Betancourt⁴⁴, F. Betti⁴², I. Bezshyiko⁴⁴, S. Bhasin⁴⁸, J. Bhowmik³⁵, L. Bianchi⁶⁷, M. S. Bieker¹⁵, N. V. Biesuz²¹, S. Bifani⁴⁷, P. Billoir¹³, A. Biolchini³², M. Birch⁵⁵, F. C. R. Bishop⁴⁹, A. Bitadze⁵⁶, A. Bizzeti⁴⁹, M. P. Blagojević⁴⁹, T. Blake⁵⁰, F. Blanc⁴³, S. Blusk⁶², D. Bobulska⁵³, J. A. Boelhave¹⁵, O. Boente Garcia¹², T. Boettcher⁵⁹, A. Boldyrev³⁸, C. S. Bolognani⁷³, N. Bondar^{38,42}, S. Borghi⁵⁶, M. Borsato¹⁷, J. T. Borsuk³⁵, S. A. Bouchiba⁴³, T. J. V. Bowcock^{42,54}, A. Boyer⁴², C. Bozzi²¹, M. J. Bradley⁵⁵, S. Braun⁶⁰, A. Brea Rodriguez⁴⁰, J. Brodzicka³⁵, A. Brosca Gonzalo⁵⁰, D. Brundu²⁷, A. Buonaura⁴⁴, L. Buonincontri²⁸, A. T. Burke⁵⁶, C. Burr⁴², A. Bursche⁶⁶, A. Butkevich³⁸, J. S. Butter³², J. Buytaert⁴², W. Byczynski⁴², S. Cadet²⁷, H. Cai⁶⁷, R. Calabrese^{21,i}, L. Caffarini^{15,13}, S. Cali²³, R. Calladine⁴⁷, M. Calvi^{26,m}, M. Calvo Gomez⁷⁴, P. Campana²³, D. H. Campora Perez⁷³, A. F. Campoverde Quezada⁶, S. Capelli^{26,m}, L. Capriotti^{20,g}, A. Carbone^{20,g}, G. Carboni³¹, R. Cardinale^{24,k}, A. Cardini²⁷, I. Carli⁴, P. Carniti^{26,m}, L. Carus¹⁴, A. Casais Vidal⁴⁰, R. Caspary¹⁷, G. Casse⁵⁴, M. Cattaneo⁴², G. Cavallero⁴², V. Cavallini^{21,i}, S. Celani⁴³, J. Cerasoli¹⁰, D. Cervenkov⁵⁷, A. J. Chadwick⁵⁴, M. G. Chapman⁴⁸, M. Charles¹³, Ph. Charpentier⁴², C. A. Chavez Barajas⁵⁴, M. Chefdeville⁸, C. Chen³, S. Chen⁴, A. Chernov³⁵, S. Chernyshenko⁴⁶, V. Chobanova⁴⁰, S. Cholak⁴³, M. Chruszcz³⁵, A. Chubykin³⁸, V. Chulikov³⁸, P. Ciambri²³, M. F. Cicala⁵⁰, X. Cid Vidal⁴⁰, G. Ciezarek⁴², G. Ciullo^{21,i}, P. E. L. Clarke⁵², M. Clemencic⁴², H. V. Cliff⁴⁹, J. Closier⁴², J. L. Cobbedick⁵⁶, V. Coco⁴², J. A. B. Coelho¹¹, J. Cogan¹⁰, E. Cogneras⁹, L. Cojocariu³⁷, P. Collins⁴², T. Colombo⁴², L. Congedo¹⁹, A. Contu²⁷, N. Cooke⁴⁷, G. Coombs⁵³, I. Corredoira⁴⁰, G. Corti⁴², B. Couturier⁴², D. C. Craik⁵⁸, J. Crkovic⁶¹, M. Cruz Torres^{1,e}, R. Currie⁵², C. L. Da Silva⁶¹, S. Dadabov³⁸, L. Dai⁶⁵, X. Dai⁵, E. Dall'Occo¹⁵, J. Dalseno⁴⁰, C. D'Ambrosio⁴², A. Danilina³⁸, P. d'Argent¹⁵, J. E. Davies⁵⁶, A. Davis⁵⁶, O. De Aguiar Francisco⁵⁶, J. de Boer⁴², K. De Bruyn⁷², S. De Capua⁵⁶, M. De Cian⁴³, U. De Freitas Carneiro Da Graça¹, E. De Lucia²³, J. M. De Miranda¹, L. De Paula², M. De Serio^{19,f}, D. De Simone⁴⁴, P. De Simone²³, F. De Vellis¹⁵, J. A. de Vries⁷³, C. T. Dean⁶¹, F. Debernardi^{19,f}, D. Decamp⁸, V. Dedu¹⁰, L. Del Buono¹³, B. Delaney⁵⁸, H.-P. Dembinski¹⁵, V. Denysenko⁴⁴, O. Deschamps⁹, F. Dettori^{27,h}, B. Dey⁷⁰, A. Di Cicco²³, P. Di Nezza²³, I. Diachkov³⁸, S. Didenko³⁸, L. Dieste Maronas⁴⁰, S. Ding⁶², V. Dobishuk⁴⁶, A. Dolmatov³⁸, C. Dong³, A. M. Donohoe¹⁸, F. Dordei²⁷, A. C. dos Reis¹, L. Douglas⁵³, A. G. Downes⁸, M. W. Dudek³⁵, L. Dufour⁴², V. Duk⁷¹, P. Durante⁴², J. M. Durham⁶¹, D. Dutta⁵⁶, A. Dziurda³⁵, A. Dzyuba³⁸, S. Easo⁵¹, U. Egede⁶³, V. Egorychev³⁸, S. Eidelman^{38,*}, C. Eirea Orro⁴⁰, S. Eisenhardt⁵², S. Ek-In⁴³, L. Eklund⁷⁵, S. Ely⁶², A. Ene³⁷, E. Eppler⁶¹, S. Escher¹⁴, J. Eschle⁴⁴, S. Esen⁴⁴, T. Evans⁵⁶, L. N. Falcao¹, Y. Fan⁶, B. Fang⁶⁷, S. Farry⁵⁴, D. Fazzini^{26,m}, M. Feo⁴², A. D. Fernez⁶⁰, F. Ferrari²⁰, L. Ferreira Lopes⁴³, F. Ferreira Rodrigues², S. Ferreres Sole³², M. Ferrillo⁴⁴, M. Ferro-Luzzi⁴², S. Filippov³⁸, R. A. Fini¹⁹, M. Fiorini^{21,i}, M. Firlej³⁴, K. M. Fischer⁵⁷, D. S. Fitzgerald⁷⁶, C. Fitzpatrick⁵⁶, T. Fiutowski³⁴, F. Fleuret¹², M. Fontana¹³, F. Fontanelli^{24,k}, R. Forty⁴², D. Foulds-Holt⁴⁹, V. Franco Lima⁵⁴, M. Franco Sevilla⁶⁰, M. Frank⁴², E. Franzoso^{21,i}, G. Frau¹⁷, C. Frei⁴², D. A. Friday⁵³, J. Fu⁶, Q. Fuehring¹⁵, E. Gabriel³², G. Galati^{19,f}, M. D. Galati⁷², A. Gallas Torreira⁴⁰, D. Galli^{20,g}, S. Gambetta^{52,42}, Y. Gan³, M. Gandelman², P. Gandini²⁵, Y. Gao⁵, M. Garau^{27,h}, L. M. Garcia Martin⁵⁰, P. Garcia Moreno³⁹, J. García Pardiñas^{26,m}, B. Garcia Plana⁴⁰, F. A. Garcia Rosales¹², L. Garrido³⁹, C. Gaspar⁴², R. E. Geertsema³², D. Gerick¹⁷, L. L. Gerken¹⁵, E. Gersabeck⁵⁶, M. Gersabeck⁵⁶, T. Gershon⁵⁰, L. Giambastiani²⁸, V. Gibson⁴⁹, H. K. Gienza³⁶, A. L. Gilman⁵⁷, M. Giovannetti^{23,t}, A. Gioventù⁴⁰, P. Gironella Gironell³⁹, C. Giugliano^{21,i}, M. A. Giza³⁵

K. Gizdov⁵², E. L. Gkougkousis⁴², V. V. Gligorov^{13,42}, C. Göbel⁶⁴, E. Golobardes⁷⁴, D. Golubkov³⁸, A. Golutvin^{55,38}, A. Gomes^{1,a}, S. Gomez Fernandez³⁹, F. Goncalves Abrantes⁵⁷, M. Goncerz³⁵, G. Gong³, I. V. Gorelov³⁸, C. Gotti²⁶, J. P. Grabowski¹⁷, T. Grammatico¹³, L. A. Granado Cardoso⁴², E. Graugés³⁹, E. Graverini⁴³, G. Graziani⁴², A. T. Grecu³⁷, L. M. Greeven³², N. A. Grieser⁴, L. Grillo⁵³, S. Gromov³⁸, B. R. Gruberg Cazon⁵⁷, C. Gu³, M. Guarise^{21,i}, M. Guittiere¹¹, P. A. Günther¹⁷, E. Gushchin³⁸, A. Guth¹⁴, Y. Guz³⁸, T. Gys⁴², T. Hadavizadeh⁶³, G. Haefeli⁴³, C. Haen⁴², J. Haimberger⁴², S. C. Haines⁴⁹, T. Halewood-leagas⁵⁴, M. M. Halvorsen⁴², P. M. Hamilton⁶⁰, J. Hammerich⁵⁴, Q. Han⁷, X. Han¹⁷, E. B. Hansen⁵⁶, S. Hansmann-Menzemer^{17,42}, L. Hao⁶, N. Harnew⁵⁷, T. Harrison⁵⁴, C. Hasse⁴², M. Hatch⁴², J. He^{6,c}, K. Heijhoff³², K. Heinicke¹⁵, C. Henderson⁵⁹, R. D. L. Henderson^{63,50}, A. M. Hennequin⁵⁸, K. Hennessy⁵⁴, L. Henry⁴², J. Heuel¹⁴, A. Hicheur², D. Hill⁴³, M. Hilton⁵⁶, S. E. Hollitt¹⁵, R. Hou⁷, Y. Hou⁸, J. Hu¹⁷, J. Hu⁶⁶, W. Hu⁵, X. Hu³, W. Huang⁶, X. Huang⁶⁷, W. Hulsbergen³², R. J. Hunter⁵⁰, M. Hushchyn³⁸, D. Hutchcroft⁵⁴, P. Ibis¹⁵, M. Idzik³⁴, D. Ilin³⁸, P. Ilten⁵⁹, A. Inglessi³⁸, A. Iniukhin³⁸, A. Ishteev³⁸, K. Ivshin³⁸, R. Jacobsson⁴², H. Jage¹⁴, S. J. Jaimes Elles⁴¹, S. Jakobsen⁴², E. Jans³², B. K. Jashal⁴¹, A. Jawahery⁶⁰, V. Jevtic¹⁵, X. Jiang^{4,6}, Y. Jiang⁶, M. John⁵⁷, D. Johnson⁵⁸, C. R. Jones⁴⁹, T. P. Jones⁵⁰, B. Jost⁴², N. Jurik⁴², I. Juszczak³⁵, S. Kandybei⁴⁵, Y. Kang³, M. Karacson⁴², D. Karpenkov³⁸, M. Karpov³⁸, J. W. Kautz⁵⁹, F. Keizer⁴², D. M. Keller⁶², M. Kenzie⁵⁰, T. Ketel³³, B. Khanji¹⁵, A. Kharisova³⁸, S. Kholodenko³⁸, T. Kim¹⁴, V. S. Kirsebom⁴³, O. Kitouni⁵⁸, S. Klaver³³, N. Kleijne^{29,q}, K. Klimaszewski³⁶, M. R. Kmiec³⁶, S. Kolliiev⁴⁶, A. Kondybayeva³⁸, A. Konoplyannikov³⁸, P. Kopciwicz³⁴, R. Kopečna¹⁷, P. Koppenburg³², M. Korolev³⁸, I. Kostyuk^{32,46}, O. Kot⁴⁶, S. Kotriakhova⁴², A. Kozachuk³⁸, P. Kravchenko³⁸, L. Kravchuk³⁸, R. D. Krawczyk⁴², M. Kreps⁵⁰, S. Kretschmar¹⁴, P. Krokovny³⁸, W. Krupa³⁴, W. Krzemien³⁶, J. Kubat¹⁷, W. Kucewicz^{35,34}, M. Kucharczyk³⁵, V. Kudryavtsev³⁸, G. J. Kunde⁶¹, A. Kupsc⁷⁵, D. Lacarrere⁴², G. Lafferty⁵⁶, A. Lai²⁷, A. Lampis^{27,h}, D. Lancierini⁴⁴, C. Landesa Gomez⁴⁰, J. J. Lane⁵⁶, R. Lane⁴⁸, G. Lanfranchi²³, C. Langenbruch¹⁴, J. Langer¹⁵, O. Lantwin³⁸, T. Latham⁵⁰, F. Lazzari^{29,u}, M. Lazzaroni^{25,1}, R. Le Gac¹⁰, S. H. Lee⁷⁶, R. Lefèvre⁹, A. Leflat³⁸, S. Legotin³⁸, P. Lenisa^{21,i}, O. Leroy¹⁰, T. Lesiak³⁵, B. Leverington¹⁷, A. Li³, H. Li⁶⁶, K. Li⁷, P. Li¹⁷, S. Li⁷, T. Li⁶⁶, Y. Li⁴, Z. Li⁶², X. Liang⁶², C. Lin⁶, T. Lin⁵¹, R. Lindner⁴², V. Lisovskyi¹⁵, R. Litvinov^{27,h}, G. Liu⁶⁶, H. Liu⁶, Q. Liu⁶, S. Liu^{4,6}, A. Lobo Salvia³⁹, A. Loi²⁷, R. Lollini⁷¹, J. Lomba Castro⁴⁰, I. Longstaff⁵³, J. H. Lopes², S. López Soliño⁴⁰, G. H. Lovell⁴⁹, Y. Lu^{4,b}, C. Lucarelli^{22,j}, D. Lucchesi^{28,o}, S. Luchuk³⁸, M. Lucio Martinez³², V. Lukashenko^{32,46}, Y. Luo³, A. Lupato⁵⁶, E. Luppi^{21,i}, A. Lusiani^{29,q}, K. Lynch¹⁸, X.-R. Lyu⁶, L. Ma⁴, R. Ma⁶, S. Maccolini²⁰, F. Machefer¹¹, F. Maciuc³⁷, V. Macko⁴³, P. Mackowiak¹⁵, S. Maddrell-Mander⁴⁸, L. R. Madhan Mohan⁴⁸, A. Maevskiy³⁸, D. Maisuzenko³⁸, M. W. Majewski³⁴, J. J. Malczewski³⁵, S. Malde⁵⁷, B. Malecki^{35,42}, A. Malinin³⁸, T. Maltsev³⁸, H. Malygina¹⁷, G. Manca^{27,h}, G. Mancinelli¹⁰, D. Manuzzi²⁰, C. A. Manzari⁴⁴, D. Marangotto^{25,1}, J. F. Marchand⁸, U. Marconi²⁰, S. Mariani^{22,j}, C. Marin Benito³⁹, M. Marinangeli⁴³, J. Marks¹⁷, A. M. Marshall⁴⁸, P. J. Marshall⁵⁴, G. Martelli^{71,p}, G. Martellotti³⁰, L. Martinazzoli^{42,m}, M. Martinelli^{26,m}, D. Martinez Santos⁴⁰, F. Martinez Vidal⁴¹, A. Massafferri¹, M. Materok¹⁴, R. Matev⁴², A. Mathad⁴⁴, V. Matiunin³⁸, C. Matteuzzi²⁶, K. R. Mattioli⁷⁶, A. Mauri³², E. Maurice¹², J. Mauricio³⁹, M. Mazurek⁴², M. McCann⁵⁵, L. Mcconnell¹⁸, T. H. McGrath⁵⁶, N. T. McHugh⁵³, A. McNab⁵⁶, R. McNulty¹⁸, J. V. Mead⁵⁴, B. Meadows⁵⁹, G. Meier¹⁵, D. Melnychuk³⁶, S. Meloni^{26,m}, M. Merk^{32,73}, A. Merli^{25,1}, L. Meyer Garcia², D. Miao^{4,6}, M. Mikhasev^{69,d}, D. A. Milanes⁶⁸, E. Millard⁵⁰, M. Milovanovic⁴², M.-N. Minard^{8,*}, A. Minotti^{26,m}, S. E. Mitchell⁵², B. Mitreska⁵⁶, D. S. Mitzel¹⁵, A. Mödden¹⁵, R. A. Mohammed⁵⁷, R. D. Moise¹⁴, S. Mokhnenko³⁸, T. Mombächer⁴⁰, I. A. Monroy⁶⁸, S. Monteil⁹, M. Morandin²⁸, G. Morello²³, M. J. Morello^{29,q}, J. Moron³⁴, A. B. Morris⁶⁹, A. G. Morris⁵⁰, R. Mountain⁶², H. Mu³, F. Muheim⁵², M. Mulder⁷², K. Müller⁴⁴, C. H. Murphy⁵⁷, D. Murray⁵⁶, R. Murta⁵⁵, P. Muzzetto^{27,h}, P. Naik⁴⁸, T. Nakada⁴³, R. Nandakumar⁵¹, T. Nanut⁴², I. Nasteva², M. Needham⁵², N. Neri^{25,1}, S. Neubert⁶⁹, N. Neufeld⁴², P. Neustroev³⁸, R. Newcombe⁵⁵, E. M. Niel⁴³, S. Nieswand¹⁴, N. Nikitin³⁸, N. S. Nolte⁵⁸, C. Normand^{8,27,h}, J. Novoa Fernandez⁴⁰, C. Nunez⁷⁶, A. Oblakowska-Mucha³⁴, V. Obraztsov³⁸, T. Oeser¹⁴, D. P. O'Hanlon⁴⁸, S. Okamura^{21,i}, R. Oldeman^{27,h}, F. Oliva⁵², M. E. Olivares⁶², C. J. G. Onderwater⁷², R. H. O'Neil⁵², J. M. Otalora Goicochea², T. Ovsiannikova³⁸, P. Owen⁴⁴, A. Oyanguen⁴¹, O. Ozcelik⁵², K. O. Padeken⁶⁹, B. Pagare⁵⁰, P. R. Pais⁴², T. Pajero⁵⁷, A. Palano¹⁹, M. Palutan²³, Y. Pan⁵⁶, G. Panshin³⁸, A. Papanestis⁵¹, M. Pappagallo^{19,f}, L. L. Pappalardo^{21,i}, C. Pappenheimer⁵⁹, W. Parker⁶⁰, C. Parkes⁵⁶, B. Passalacqua^{21,i}, G. Passaleva²², A. Pastore¹⁹, M. Patel⁵⁵, C. Patrignani^{20,g}, C. J. Pawley⁷³, A. Pearce⁴²,

A. Pellegrino³², M. Pepe Altarelli⁴², S. Perazzini²⁰, D. Pereima³⁸, A. Pereiro Castro⁴⁰, P. Perret⁹, M. Petric⁵³, K. Petridis⁴⁸, A. Petrolini^{24.k}, A. Petrov³⁸, S. Petrucci⁵², M. Petruzzo²⁵, H. Pham⁶², A. Philippov³⁸, R. Piandani⁶, L. Pica^{29.q}, M. Piccini⁷¹, B. Pietrzyk⁸, G. Pietrzyk¹¹, M. Pili⁵⁷, D. Pinci³⁰, F. Pisani⁴², M. Pizzichemi^{26.42.m}, V. Placinta³⁷, J. Plews⁴⁷, M. Plo Casasus⁴⁰, F. Polci^{13.42}, M. Poli Lener²³, M. Poliakov⁶², A. Poluektov¹⁰, N. Polukhina³⁸, I. Polyakov⁴², E. Polycarpo², S. Ponce⁴², D. Popov^{6.42}, S. Popov³⁸, S. Poslavskii³⁸, K. Prasanth³⁵, L. Promberger⁴², C. Prouve⁴⁰, V. Pugatch⁴⁶, V. Puill¹¹, G. Punzi^{29.r}, H. R. Qi³, W. Qian⁶, N. Qin³, S. Qu³, R. Quagliani⁴³, N. V. Raab¹⁸, R. I. Rabadan Trejo⁶, B. Rachwal³⁴, J. H. Rademacker⁴⁸, R. Rajagopalan⁶², M. Rama²⁹, M. Ramos Pernas⁵⁰, M. S. Rangel², F. Ratnikov³⁸, G. Raven^{33.42}, M. Rebollo De Miguel⁴¹, F. Redi⁴², J. Reich⁴⁸, F. Reiss⁵⁶, C. Remon Alepuz⁴¹, Z. Ren³, V. Renaudin⁵⁷, P. K. Resmi¹⁰, R. Ribatti^{29.q}, A. M. Ricci²⁷, S. Ricciardi⁵¹, K. Richardson⁵⁸, M. Richardson-Slipper⁵², K. Rinnert⁵⁴, P. Robbe¹¹, G. Robertson⁵², A. B. Rodrigues⁴³, E. Rodrigues⁵⁴, J. A. Rodriguez Lopez⁶⁸, E. Rodriguez Rodriguez⁴⁰, A. Rollings⁵⁷, P. Roloff⁴², V. Romanovskiy³⁸, M. Romero Lamas⁴⁰, A. Romero Vidal⁴⁰, J. D. Roth^{76.*}, M. Rotondo²³, M. S. Rudolph⁶², T. Ruf⁴², R. A. Ruiz Fernandez⁴⁰, J. Ruiz Vidal⁴¹, A. Ryzhikov³⁸, J. Ryzka³⁴, J. J. Saborido Silva⁴⁰, N. Sagidova³⁸, N. Sahoo⁴⁷, B. Saitta^{27.h}, M. Salomoni⁴², C. Sanchez Gras³², I. Sanderswood⁴¹, R. Santacesaria³⁰, C. Santamarina Rios⁴⁰, M. Santimaria²³, E. Santovetti^{31.t}, D. Saranin³⁸, G. Sarpis¹⁴, M. Sarpis⁶⁹, A. Sarti³⁰, C. Satriano^{30.s}, A. Satta³¹, M. Saur¹⁵, D. Savrina³⁸, H. Sazak⁹, L. G. Scantlebury Smead⁵⁷, A. Scarabotto¹³, S. Schael¹⁴, S. Scherl⁵⁴, M. Schiller⁵³, H. Schindler⁴², M. Schmelling¹⁶, B. Schmidt⁴², S. Schmitt¹⁴, O. Schneider⁴³, A. Schopper⁴², M. Schubiger³², S. Schulte⁴³, M. H. Schune¹¹, R. Schwemmer⁴², B. Sciascia^{23.42}, A. Sciuccati⁴², S. Sellam⁴⁰, A. Semennikov³⁸, M. Senghi Soares³³, A. Sergi^{24.k}, N. Serra⁴⁴, L. Sestini²⁸, A. Seuthe¹⁵, Y. Shang⁵, D. M. Shangase⁷⁶, M. Shapkin³⁸, I. Shchemerov³⁸, L. Shchutka⁴³, T. Shears⁵⁴, L. Shekhtman³⁸, Z. Shen⁵, S. Sheng^{4.6}, V. Shevchenko³⁸, B. Shi⁶, E. B. Shields^{26.m}, Y. Shimizu¹¹, E. Shmanin³⁸, J. D. Shupperd⁶², B. G. Siddi^{21.i}, R. Silva Coutinho⁴⁴, G. Simi²⁸, S. Simone^{19.f}, M. Singla⁶³, N. Skidmore⁵⁶, R. Skuza¹⁷, T. Skwarnicki⁶², M. W. Slater⁴⁷, J. C. Smallwood⁵⁷, J. G. Smeaton⁴⁹, E. Smith⁴⁴, K. Smith⁶¹, M. Smith⁵⁵, A. Snoch³², L. Soares Lavra⁹, M. D. Sokoloff⁵⁹, F. J. P. Soler⁵³, A. Solomin^{38.48}, A. Solovov³⁸, I. Solovyevev³⁸, F. L. Souza De Almeida², B. Souza De Paula², B. Spaan^{15.*}, E. Spadaro Norella^{25.1}, E. Spiridenkov³⁸, P. Spradlin⁵³, V. Sriskaran⁴², F. Stagni⁴², M. Stahl⁵⁹, S. Stahl⁴², S. Stanislaus⁵⁷, E. N. Stein⁴², O. Steinkamp⁴⁴, O. Stenyakin³⁸, H. Stevens¹⁵, S. Stone^{62.*}, D. Strelakina³⁸, F. Suljik⁵⁷, J. Sun²⁷, L. Sun⁶⁷, Y. Sun⁶⁰, P. Svihra⁵⁶, P. N. Swallow⁴⁷, K. Swientek³⁴, A. Szabelski³⁶, T. Szumlak³⁴, M. Szymanski⁴², Y. Tan³, S. Taneja⁵⁶, A. R. Tanner⁴⁸, M. D. Tat⁵⁷, A. Terentev³⁸, F. Teubert⁴², E. Thomas⁴², D. J. D. Thompson⁴⁷, K. A. Thomson⁵⁴, H. Tilquin⁵⁵, V. Tisserand⁹, S. T'Jampens⁸, M. Tobin⁴, L. Tomassetti^{21.i}, G. Tonani^{25.1}, X. Tong⁵, D. Torres Machado¹, D. Y. Tou³, E. Trifonova³⁸, S. M. Trilov⁴⁸, C. Trippel⁴³, G. Tuci⁶, A. Tully⁴³, N. Tuning^{32.42}, A. Ukleja³⁶, D. J. Unverzagt¹⁷, E. Ursov³⁸, A. Usachov³², A. Ustyuzhanin³⁸, U. Uwer¹⁷, A. Vagner³⁸, V. Vagnoni²⁰, A. Valassi⁴², G. Valenti²⁰, N. Valls Canudas⁷⁴, M. van Beuzekom³², M. Van Dijk⁴³, H. Van Hecke⁶¹, E. van Herwijnen³⁸, C. B. Van Hulse^{40.w}, M. van Veghel⁷², R. Vazquez Gomez³⁹, P. Vazquez Regueiro⁴⁰, C. Vázquez Sierra⁴², S. Vecchi²¹, J. J. Velthuis⁴⁸, M. Veltri^{22.v}, A. Venkateswaran⁶², M. Veronesi³², M. Vesterinen⁵⁰, D. Vieira⁵⁹, M. Vieites Diaz⁴³, X. Vilasis-Cardona⁷⁴, E. Vilella Figueras⁵⁴, A. Villa²⁰, P. Vincent¹³, F. C. Volle¹¹, D. vom Bruch¹⁰, A. Vorobyev³⁸, V. Vorobyev³⁸, N. Voropaev³⁸, K. Vos⁷³, C. Vrahas⁵², R. Waldi¹⁷, J. Walsh²⁹, G. Wan⁵, C. Wang¹⁷, J. Wang⁵, J. Wang⁴, J. Wang³, J. Wang⁶⁷, M. Wang⁵, R. Wang⁴⁸, X. Wang⁶⁶, Y. Wang⁷, Z. Wang⁴⁴, Z. Wang³, Z. Wang⁶, J. A. Ward^{50.63}, N. K. Watson⁴⁷, D. Websdale⁵⁵, Y. Wei⁵, C. Weisser⁵⁸, B. D. C. Westhenry⁴⁸, D. J. White⁵⁶, M. Whitehead⁵³, A. R. Wiederhold⁵⁰, D. Wiedner¹⁵, G. Wilkinson⁵⁷, M. K. Wilkinson⁵⁹, I. Williams⁴⁹, M. Williams⁵⁸, M. R. J. Williams⁵², R. Williams⁴⁹, F. F. Wilson⁵¹, W. Wislicki³⁶, M. Witek³⁵, L. Witola¹⁷, C. P. Wong⁶¹, G. Wormser¹¹, S. A. Wotton⁴⁹, H. Wu⁶², K. Wyllie⁴², Z. Xiang⁶, D. Xiao⁷, Y. Xie⁷, A. Xu⁵, J. Xu⁶, L. Xu³, L. Xu³, M. Xu⁵⁰, Q. Xu⁶, Z. Xu⁹, Z. Xu⁶, D. Yang³, S. Yang⁶, Y. Yang⁶, Z. Yang⁵, Z. Yang⁶⁰, L. E. Yeomans⁵⁴, H. Yin⁷, J. Yu⁶⁵, X. Yuan⁶², E. Zaffaroni⁴³, M. Zavertyaev¹⁶, M. Zdybal³⁵, O. Zenaiev⁴², M. Zeng³, C. Zhang⁵, D. Zhang⁷, L. Zhang³, S. Zhang⁶⁵, S. Zhang⁵, Y. Zhang⁵, Y. Zhang⁵⁷, A. Zharkova³⁸, A. Zhelezov¹⁷, Y. Zheng⁶, T. Zhou⁵, X. Zhou⁶, Y. Zhou⁶, V. Zhovkovska¹¹, X. Zhu³, X. Zhu⁷, Z. Zhu⁶, V. Zhukov^{14.38}, Q. Zou^{4.6}, S. Zucchelli^{20.g}, D. Zuliani²⁸, G. Zunica⁵⁶

¹ Centro Brasileiro de Pesquisas Físicas (CBPF), Rio de Janeiro, Brazil

² Universidade Federal do Rio de Janeiro (UFRJ), Rio de Janeiro, Brazil

- ³ Center for High Energy Physics, Tsinghua University, Beijing, China
- ⁴ Institute Of High Energy Physics (IHEP), Beijing, China
- ⁵ School of Physics State Key Laboratory of Nuclear Physics and Technology, Peking University, Beijing, China
- ⁶ University of Chinese Academy of Sciences, Beijing, China
- ⁷ Institute of Particle Physics, Central China Normal University, Wuhan, Hubei, China
- ⁸ CNRS, IN2P3-LAPP, Université Savoie Mont Blanc, Annecy, France
- ⁹ CNRS/IN2P3, LPC, Université Clermont Auvergne, Clermont-Ferrand, France
- ¹⁰ CNRS/IN2P3, CPPM, Aix Marseille Univ, Marseille, France
- ¹¹ CNRS/IN2P3, IJCLab, Université Paris-Saclay, Orsay, France
- ¹² Laboratoire Leprince-Ringuet, CNRS/IN2P3, Ecole Polytechnique, Institut Polytechnique de Paris, Palaiseau, France
- ¹³ LPNHE, CNRS/IN2P3, Sorbonne Université, Paris Diderot Sorbonne Paris Cité, Paris, France
- ¹⁴ I. Physikalisches Institut, RWTH Aachen University, Aachen, Germany
- ¹⁵ Fakultät Physik, Technische Universität Dortmund, Dortmund, Germany
- ¹⁶ Max-Planck-Institut für Kernphysik (MPIK), Heidelberg, Germany
- ¹⁷ Physikalisches Institut, Ruprecht-Karls-Universität Heidelberg, Heidelberg, Germany
- ¹⁸ School of Physics, University College Dublin, Dublin, Ireland
- ¹⁹ INFN Sezione di Bari, Bari, Italy
- ²⁰ INFN Sezione di Bologna, Bologna, Italy
- ²¹ INFN Sezione di Ferrara, Ferrara, Italy
- ²² INFN Sezione di Firenze, Firenze, Italy
- ²³ INFN Laboratori Nazionali di Frascati, Frascati, Italy
- ²⁴ INFN Sezione di Genova, Genoa, Italy
- ²⁵ INFN Sezione di Milano, Milan, Italy
- ²⁶ INFN Sezione di Milano-Bicocca, Milan, Italy
- ²⁷ INFN Sezione di Cagliari, Monserrato, Italy
- ²⁸ Università degli Studi di Padova, Università e INFN, Padova, Padua, Italy
- ²⁹ INFN Sezione di Pisa, Pisa, Italy
- ³⁰ INFN Sezione di Roma La Sapienza, Rome, Italy
- ³¹ INFN Sezione di Roma Tor Vergata, Rome, Italy
- ³² Nikhef National Institute for Subatomic Physics, Amsterdam, The Netherlands
- ³³ Nikhef National Institute for Subatomic Physics and VU University Amsterdam, Amsterdam, The Netherlands
- ³⁴ Faculty of Physics and Applied Computer Science, AGH-University of Science and Technology, Kraków, Poland
- ³⁵ Henryk Niewodniczanski Institute of Nuclear Physics, Polish Academy of Sciences, Kraków, Poland
- ³⁶ National Center for Nuclear Research (NCBJ), Warsaw, Poland
- ³⁷ Horia Hulubei National Institute of Physics and Nuclear Engineering, Bucharest-Magurele, Romania
- ³⁸ Affiliated with an Institute Covered by a Cooperation Agreement with CERN, Geneva, Switzerland
- ³⁹ ICCUB, Universitat de Barcelona, Barcelona, Spain
- ⁴⁰ Instituto Galego de Física de Altas Enerxías (IGFAE), Universidade de Santiago de Compostela, Santiago de Compostela, Spain
- ⁴¹ Instituto de Física Corpuscular, Centro Mixto Universidad de Valencia-CSIC, Valencia, Spain
- ⁴² European Organization for Nuclear Research (CERN), Geneva, Switzerland
- ⁴³ Institute of Physics, Ecole Polytechnique Fédérale de Lausanne (EPFL), Lausanne, Switzerland
- ⁴⁴ Physik-Institut, Universität Zürich, Zurich, Switzerland
- ⁴⁵ NSC Kharkiv Institute of Physics and Technology (NSC KIPT), Kharkiv, Ukraine
- ⁴⁶ Institute for Nuclear Research of the National Academy of Sciences (KINR), Kyiv, Ukraine
- ⁴⁷ University of Birmingham, Birmingham, UK
- ⁴⁸ H.H. Wills Physics Laboratory, University of Bristol, Bristol, UK
- ⁴⁹ Cavendish Laboratory, University of Cambridge, Cambridge, UK
- ⁵⁰ Department of Physics, University of Warwick, Coventry, UK
- ⁵¹ STFC Rutherford Appleton Laboratory, Didcot, UK
- ⁵² School of Physics and Astronomy, University of Edinburgh, Edinburgh, UK
- ⁵³ School of Physics and Astronomy, University of Glasgow, Glasgow, UK
- ⁵⁴ Oliver Lodge Laboratory, University of Liverpool, Liverpool, UK

- ⁵⁵ Imperial College London, London, UK
⁵⁶ Department of Physics and Astronomy, University of Manchester, Manchester, UK
⁵⁷ Department of Physics, University of Oxford, Oxford, UK
⁵⁸ Massachusetts Institute of Technology, Cambridge, MA, USA
⁵⁹ University of Cincinnati, Cincinnati, OH, USA
⁶⁰ University of Maryland, College Park, MD, USA
⁶¹ Los Alamos National Laboratory (LANL), Los Alamos, NM, USA
⁶² Syracuse University, Syracuse, NY, USA
⁶³ School of Physics and Astronomy, Monash University, Melbourne, Australia, associated to ⁵⁰
⁶⁴ Pontifícia Universidade Católica do Rio de Janeiro (PUC-Rio), Rio de Janeiro, Brazil, associated to ²
⁶⁵ Physics and Micro Electronic College, Hunan University, Changsha, China, associated to ⁷
⁶⁶ Guangdong Provincial Key Laboratory of Nuclear Science, Guangdong-Hong Kong Joint Laboratory of Quantum Matter, Institute of Quantum Matter, South China Normal University, Guangzhou, China, associated to ³
⁶⁷ School of Physics and Technology, Wuhan University, Wuhan, China, associated to ³
⁶⁸ Departamento de Física, Universidad Nacional de Colombia, Bogotá, Colombia, associated to ¹³
⁶⁹ Helmholtz-Institut für Strahlen und Kernphysik, Universität Bonn, Bonn, Germany, associated to ¹⁷
⁷⁰ Eotvos Lorand University, Budapest, Hungary, associated to ⁴²
⁷¹ INFN Sezione di Perugia, Perugia, Italy, associated to ²¹
⁷² Van Swinderen Institute, University of Groningen, Groningen, The Netherlands, associated to ³²
⁷³ Universiteit Maastricht, Maastricht, The Netherlands, associated to ³²
⁷⁴ DS4DS, La Salle, Universitat Ramon Llull, Barcelona, Spain, associated to ³⁹
⁷⁵ Department of Physics and Astronomy, Uppsala University, Uppsala, Sweden, associated to ⁵³
⁷⁶ University of Michigan, Ann Arbor, MI, USA, associated to ⁶²

^a Also at Universidade de Brasília, Brasília, Brazil

^b Also at Central South U., Changsha, China

^c Also at Hangzhou Institute for Advanced Study, UCAS, Hangzhou, China

^d Also at Excellence Cluster ORIGINS, Munich, Germany

^e Also at Universidad Nacional Autónoma de Honduras, Tegucigalpa, Honduras

^f Also at Università di Bari, Bari, Italy

^g Also at Università di Bologna, Bologna, Italy

^h Also at Università di Cagliari, Cagliari, Italy

ⁱ Also at Università di Ferrara, Ferrara, Italy

^j Also at Università di Firenze, Firenze, Italy

^k Also at Università di Genova, Genoa, Italy

^l Also at Università degli Studi di Milano, Milan, Italy

^m Also at Università di Milano Bicocca, Milan, Italy

ⁿ Also at Università di Modena e Reggio Emilia, Modena, Italy

^o Also at Università di Padova, Padua, Italy

^p Also at Università di Perugia, Perugia, Italy

^q Also at Scuola Normale Superiore, Pisa, Italy

^r Also at Università di Pisa, Pisa, Italy

^s Also at Università della Basilicata, Potenza, Italy

^t Also at Università di Roma Tor Vergata, Rome, Italy

^u Also at Università di Siena, Siena, Italy

^v Also at Università di Urbino, Urbino, Italy

^w Also at Universidad de Alcalá, Alcalá de Henares, Spain

*Deceased